Ambiguity in antiproton-nucleus potentials from antiprotonic-atom data

Cheuk-Yin Wong* and A. K. Kerman
Center for Theoretical Physics, Massachusetts Institute of Technology, Cambridge, Massachusetts 02139

G. R. Satchler and A. D. MacKellar†
Oak Ridge National Laboratory, Oak Ridge, Tennessee 37830
(Received 19 September 1983)

We show that the $\bar{p}$-atomic data for $\bar{p}+{}^{12}C$, ${}^{16}O$, S, and ${}^{89}Y$ do not yield unique $\bar{p}$-nucleus potentials. Two families of potentials are found, one with shallow imaginary and deep real parts and one with deep imaginary and shallow real parts. We examine some possible consequences for the n-$\bar{n}$ oscillation time, for $\bar{p}$-nuclear bound states, and for $\bar{p}$-nucleus scattering.

I. INTRODUCTION

There has been much interest recently[1-4] in obtaining information about the $\bar{p}$-nucleus optical potential from data on the widths and energy shifts of the atomic levels of $\bar{p}$-nucleus systems. Some authors have constructed theoretical potentials, either derived from some nucleon-antinucleon interaction model,[5,6] or based upon a relativistic mean field approach.[7] Others[1-4] have used phenomenological potentials, usually assumed to be proportional to the density distribution of the nucleus, whose real and imaginary strengths are then adjusted to fit the $\bar{p}$-atom data. We wish to emphasize that the latter procedure does not result in unambiguous potential parameters. We show that the presently available $\bar{p}$-atom data for ${}^{12}C$, ${}^{16}O$, S, and ${}^{89}Y$ are consistent with at least two discrete families of potentials. One family has a real well depth V of order 100 MeV and a deep imaginary part W of order 100—200 MeV. This family, which we shall call D, corresponds to the results quoted from previous analyses.[1-4] The other family, that we shall call S, has a much more shallow imaginary potential with $W\sim 15-45$ MeV, associated with a deep real potential with $V\sim 200-350$ MeV.

We also discuss the implications of this potential ambiguity for other $\bar{p}$ phenomena. Knowledge of the $\bar{p}$ optical potential throws light on the $\bar{n}$ optical potential, which itself has some influence on estimates[9,10] of the n-$\bar{n}$ oscillation time and its consequent observation. Further, the character of the nuclear potential determines whether there exist observable bound states for antiprotons *within* the nucleus ($\bar{p}$-nuclear states rather than $\bar{p}$—atomic states). Finally, the potentials obtained for negative energy $\bar{p}$-states may provide some hints concerning the potentials which are appropriate for $\bar{p}$-nucleus scattering.

II. ANALYSIS OF $\bar{p}$-ATOM DATA

Four representative cases, $\bar{p}+{}^{12}C$, ${}^{16}O$, S, and ${}^{89}Y$, were chosen from those few for which data are available[1-4,11] for all three quantities ϵ, Γ, and Γ'. The quantities ϵ and Γ are the shift and the width of the x-ray transition to the lowest observed atomic state $|Nl\rangle$ owing to the presence of the strong interaction. As the perturbation of the higher initial state $|N+1,l+1\rangle$ is very small, it is a good assumption that the shift and width of the radiative transition arise entirely from those of the final state. The quantities $-\epsilon$, and Γ are then the energy shift and width of the lowest observed atomic state $|Nl\rangle$ owing to the nuclear potential. The quantities ϵ' and Γ' are the energy shift and the width of the initial state $|N+1,l+1\rangle$. The calculated values in Table I verify that $\Gamma'\ll\Gamma$ and $|\epsilon'|\ll|\epsilon|$.

There is considerable uncertainty about the detailed shape of the antiproton optical potential, but we follow several previous authors[1-4] in assuming that it is similar to the shape of the nuclear density distribution,

$$U(r)=-V\frac{1+w(r/c)^2}{1+\exp[(r-c)/a_V]}-iW\frac{1+w(r/c)^2}{1+\exp[(r-c)/a_W]}\ , \tag{1}$$

where the radius c, the diffuseness a, and the parameter w are taken from analyses of electron scattering, with some minor increases in the diffuseness parameters to account approximately for the finite range of the underlying $N\bar{N}$ interaction.[12] The parameter values used are included in Table I.

The nuclear potential (1), together with the Coulomb potential, were inserted in a nonrelativistic Schrödinger equation and the complex eigenvalues for bound states were obtained (see the Appendix). The imaginary part gives the width Γ, and comparison of the real part with the real eigenvalue obtained with the Coulomb potential alone gives the energy shift ϵ. Strengths V and W were then found which gave the observed most probable values of ϵ and Γ. There are many such discrete pairs of (V,W), corresponding to states with the same energy and width but whose wave functions (both real and imaginary parts) have different numbers of radial nodes within the nuclear potential. The pairs of (V,W) chosen were those which best reproduced the observed width Γ' of the next higher atomic level.

Except for ${}^{16}O$, where a possible third candidate (called S') was found, this procedure led to two acceptable pairs

TABLE I. Results of optical potential analyses of the $\bar{p}$-atom data shown.

Nucleus	^{12}C[a]	^{16}O[a]	S[b]	^{89}Y[a]
Shape				
c (fm)	2.355	2.608	3.458	4.860
a_V (fm)	0.548	0.539	0.632	0.567
a_W (fm)	0.527	0.518	0.614	0.546
w	−0.149	−0.051	−0.208	0
S type				
V (MeV)	296	198	304	358
W (MeV)	44	30	30.5	15
Γ' (eV)	0.03	0.59	3.38	7.97
ϵ' (eV)	0.01	0.41	0.97	9.32
D type				
V (MeV)	127	86	128	66
W (MeV)	119	161	115	212
Γ' (eV)	0.015	0.66	1.35	9.20
ϵ' (eV)	0.002	0.02	0.06	−0.31
Experimental				
ϵ (eV)	−4±10	−111±53	−70±41	−150±160
Γ (eV)	42±18	484±222	570±190	800±320
Γ' (eV)	$0.0365^{+0.015}_{-0.011}$	0.64±0.11	3.0 ±0.7	$6.8^{+1.9}_{-1.4}$

[a]Data from Ref. 2.
[b]Combined data from Refs. 3 and 11.

of (V,W), given in Table I. One set is characterized by a deep (D) absorptive potential ($W\sim115-210$ MeV) and a relatively shallow real potential ($V\sim65-130$ MeV), while the other is characterized by a shallow (S) absorptive and a deep real potential ($W\sim15-45$ MeV, $V\sim200-360$ MeV). In both sets the smaller W tends to be associated with the larger V and vice versa. Also, we see from Table I that while the S sets predict satisfactory values of Γ' in each case, those predicted by the D sets for ^{12}C and S are rather too small. It is the D type of potential, with $W\sim200$ MeV, that has been deduced by previous analyses of this kind.[2-4]

In order to give some estimate of the uncertainties associated with the V and W parameters owing to statistical uncertainties in the data, the procedure was repeated, obtaining V and W for the most probable value of ϵ together with plus or minus one standard deviation on the value of Γ, and then for the most probable Γ with plus or minus one standard deviation for ϵ. The results, together with the most probable values from Table I, are shown plotted in the V,W plane in Fig. 1. It is seen that the S sets (lower case W) are the best determined.

The value of $V\approx200$ MeV for the S set for ^{16}O is smaller than the values ($\gtrsim300$ MeV) for the other three nuclei (Table I). There is, however, another potential which we call S' that reproduces ϵ and Γ for ^{16}O which has $V=367$ MeV and $W=34$ MeV, although this yields $\Gamma'=1.2$ eV, somewhat larger than the experimental value.

To give some indication of the sensitivity of the results to the choice of density distribution parameters [i.e., the values of c and a in Eq. (1) for the potential], we compare in Table II the V and W obtained for ^{16}O with our choice and with two other parameter sets used elsewhere.[2,10] We see that although the precise numbers depend upon the choice, two acceptable solutions S and D occur, and the ambiguity remains.

The way the two potential families can give the same widths Γ is easily understood. The stronger attraction owing to the deep real well of the S type leads to a larger wave function amplitude within the nucleus, as well as introducing an extra radial node, and hence requires a weak-

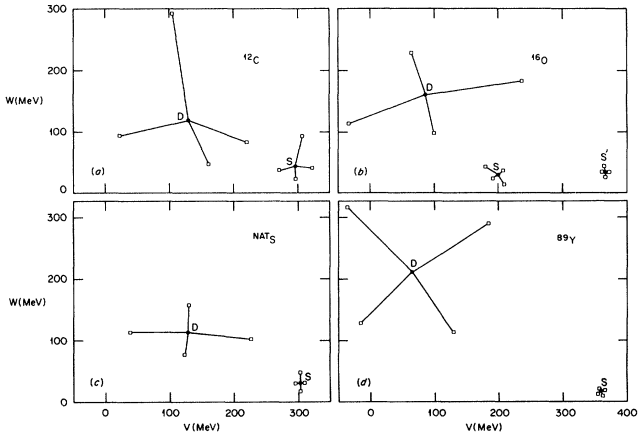

FIG. 1. Real (V) and imaginary (W) potential depths which reproduce the experimental shifts ϵ and widths Γ given in Table I. The solid dots correspond to the most probable measured values, while the open squares were obtained using plus or minus one standard deviation.

TABLE II. Values of V and W of the optical potential obtained from the analysis of $\bar{p}+^{16}O$ atomic data given in Table I, making three different assumptions for the radius and diffuseness parameters. The values of ϵ' and Γ' are also listed.

	Shape				S type				D type			
	c (fm)	a_v (fm)	a_W (fm)	w	V (MeV)	W (MeV)	ϵ' (eV)	Γ' (eV)	V (MeV)	W (MeV)	ϵ' (eV)	Γ' (eV)
I[a]	2.60	0.50	0.50	0	191	32.2	0.34	0.50	110	176	0.02	0.66
II[a]	2.44	0.523	0.523	0	208	31.3	0.36	0.42	109	207	0.02	0.67
III[b]	2.618	0.539	0.518	−0.051	198	30.4	0.41	0.59	86	161	0.02	0.66

[a]From Ref. 10.
[b]Present work.

er absorptive potential to produce a given width. This is illustrated in Fig. 2, which shows the (complex) radial wave functions $u(r)=r\psi(r)$ in the interior of the nucleus, for the $3d$ state of the $\bar{p}+^{16}O$ atom, for the two types of potential. The wave functions have been normalized according to

$$\int d\vec{r}\,\psi_\lambda(r)Y^*_{l_\lambda m_\lambda}(\theta\phi)\psi_\mu(r)Y_{l_\mu m_\mu}(\theta\phi)=\delta(\lambda l_\lambda m_\lambda,\mu l_\mu m_\mu)\ .$$

(Note that in this case there is no complex conjugation of the radial wave function.) The S-type potential gives larger amplitudes at small radii than the D type, although outside the nuclear potential ($r\gtrsim 6$ fm) the two wave functions are identical.

It is also of interest to see the approximate location of annihilation for the two potential types. Figure 3 shows an example of the product $-\mathrm{Im}U(r)\,|\,\psi(r)\,|^2$ for the $3d$ atomic state for $\bar{p}+^{16}O$; this gives the probability of annihilation per unit volume at the radius r. This peaks at $r\approx 1.1$ fm for the S potential, well inside the ^{16}O nucleus, whereas annihilation is strongest in the outer surface, $r\approx 3.3$ fm, for the D potential. Of course, the integral of this quantity is the same for the two potentials because they were chosen to give the same width for the atomic level.

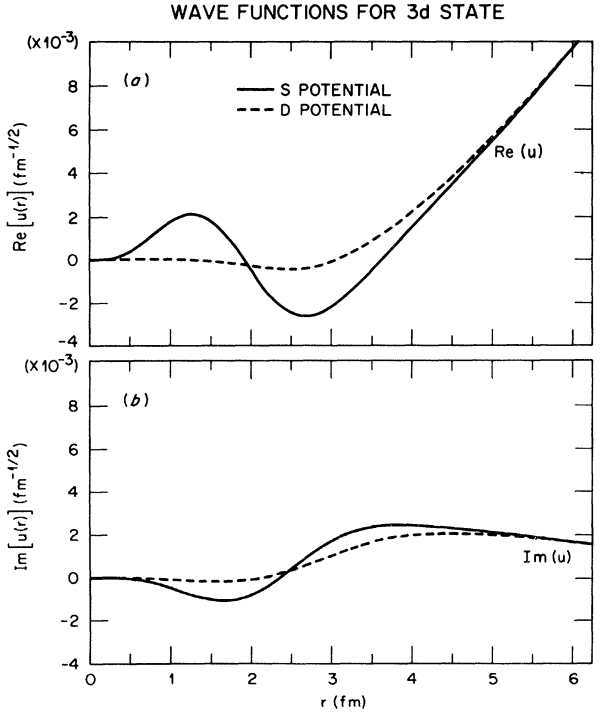

FIG. 2. Radial wave functions $u(r)=r\psi(r)$ in the vicinity of the nucleus for the $\bar{p}+^{16}O$ atomic $3d$ state, for the S- and D-type potentials of Table I.

III. DISCUSSION

A. The $\bar{p}$-atom results and other potentials

The $\bar{p}$-atom data provide two numbers, ϵ and Γ, with which to determine the complex $\bar{p}$-nucleus potential, with some additional constraint provided by the third datum Γ'. Clearly these are insufficient to determine the potential fully, and, following previous authors,[1–4] we have chosen the potential shape (1) to follow the shape of the nuclear density distribution, thus leaving two strength parameters V and W to be fixed by the measurements. Within this context, we have demonstrated a discrete ambiguity in which at least two sets of (V,W) are compatible with the data. Below, we explore possible consequences for other measurements, but the present $\bar{p}$-atom data alone cannot distinguish between them. Further, the experimental uncertainties (often large) associated with these data result in relatively large regions of continuous ambiguity around each most probable point in the parameter space (see Fig. 1).

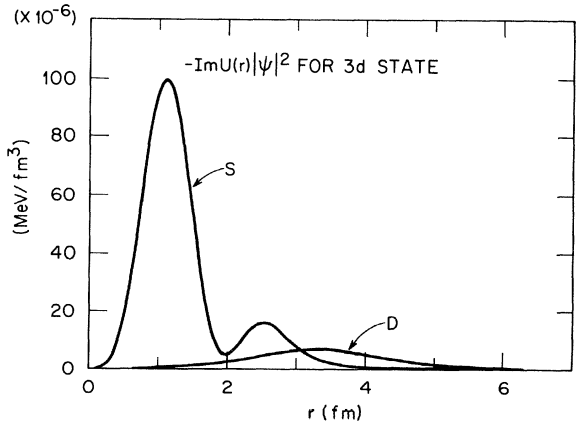

FIG. 3. Probability of annihilation per unit volume at the radius r for the atomic $3d$ state of $\bar{p}+^{16}O$, given by the quantity $-\mathrm{Im}U(r)\,|\,\psi(r)\,|^2$ for the S- and D-type potentials of Table I.

In addition, the potential form (1), with c and a taken from charge density measurements, was only adopted for simplicity. There are indications from theoretical studies[5,6] that the effective $N\bar{N}$ interaction is strongly density dependent, resulting in $\bar{N}$-nucleus potential shapes considerably different from those of the nuclear density and with real and imaginary parts having considerably different shapes. Indeed, this work[5,6] suggests a real potential which is attractive in the interior but with a repulsive barrier of some 10 MeV at the surface. Apparently these potentials are not incompatible with the $\bar{p}$-atom data. Further, although the differences in shape make a direct comparison with our results difficult, these theoretical potentials have imaginary parts that are much deeper than their real ones and hence are more like our D potentials.

On the other hand, the relativistic mean field approach[7,8] predicts *very* deep attractive real potentials ($V \sim 700$ MeV). These potentials roughly follow the corresponding nuclear density distributions except for a small increase in diffuseness; consequently they are similar in shape to the ones used here. The present form of the theory ignores the presence of annihilation and thus only provides the real part of the potential; the imaginary part has to be constructed independently. One wonders whether dispersive corrections associated with the strong absorption owing to annihilation would not also produce a large modification of the real potential. It also ignores the effects of density dependence and vacuum fluctuation which may reduce the real part of the potential.

B. Implications for neutron-antineutron oscillations in nuclei

If the baryon-number-violating interaction within a nucleus is the same as in free space, it can be shown[9,10] that the effective mean lifetime τ_A for annihilation of a neutron in nuclear matter, owing to n-$\bar{n}$ oscillations, is given by

$$\tau_A = \tau_{n\bar{n}}^2 \frac{(V_{\bar{n}} - V_n)^2 + W_{\bar{n}}^2}{2\hbar W_{\bar{n}}} , \tag{2}$$

where $\tau_{n\bar{n}}$ is the n-$\bar{n}$ oscillation time, $V_{\bar{n}}$ and $W_{\bar{n}}$ are the real and imaginary strengths of the $\bar{n}$ optical potential, and V_n is the real strength of the n optical potential. In a finite nucleus, it is a reasonable approximation to replace $W_{\bar{n}}$ in Eq. (2) by the averaged quantity

$$\langle W_{\bar{n}} \rangle = -\int \mathrm{Im}U(r)\rho(r)r^2 dr \Big/ \int \rho(r) r^2 dr ,$$

where $\rho(r)$ is the density distribution, and similarly for V. For a small nucleus like ^{16}O, the averaged quantities are approximately one-half the corresponding well depths. Consequently the estimate of τ_A in such cases is only about one-half the value that would be obtained by simply using the well depths in Eq. (2).

Using the $\bar{p}$ potentials for ^{16}O found in the present work as approximations to the $\bar{n}$ potential, and taking a real neutron potential of depth 71.5 MeV,[10] the effective lifetime τ_A is longer for the potential family S than for the family D. Alternatively, using the limit $\tau_A \geq 1.4 \times 10^{30}$ y placed on this time by the observed stability of ^{16}O,[13] the S potentials imply a lower limit on the n-$\bar{n}$ oscillation time that is several times smaller than that obtained using the D potentials (Table III).

C. Antiproton nuclear states

The $\bar{p}$-atomic states are bound by the Coulomb field, with the nuclear interaction acting as a perturbation. There may also be "nuclear" states where the antiproton is bound within the nucleus; the absorption owing to annihilation will result in large widths of order $2\langle W \rangle$. Here we consider differences between such states predicted by the two sets of potentials obtained in the present work. The D family of potentials has $W \sim 100-200$ MeV and of the same order as V. Consequently we expect the $\bar{p}$-nuclear states to be so broad as to be unobservable. However, the situation is more favorable for the S family.

The single-particle levels of $\bar{p} + {}^{16}$O obtained using the S potential of Table I are shown in Fig. 4, and their widths given. Spin-orbit coupling is ignored. The states are labeled $[n]l$ to emphasize the use here of the nuclear convention for the principal quantum number n, in contrast to the atomic states labeled Nl, where $N = n + l + 1$ and n is the number of radial nodes (excluding the origin and infinity). The nuclear states have roughly equal spacings "$\hbar\omega$" ~ 35 MeV. The lowest, $[0]s$, state has a width of about 54 MeV. The highest group of bound states, $[2]s$, $[1]d$, and $[0]g$, are only one-half as broad; their greater spatial extent provides less overlap with the absorptive potential.

The atomic states have binding energies from 0 to -0.4 MeV. The last observed transition in the atomic cascade is that which leaves the $\bar{p} + {}^{16}$O system in the $3d$ state. This may then decay by annihilation ($\Gamma \approx 480$ eV) or by making a further transition to the atomic $2p$ state or one of the nuclear states. An $E1$ decay would lead to the $[1]p$, $[0]f$, or $[0]p$ state. The partial widths for these decays were calculated and are given in Table IV. Although the wave function overlap between atomic and nuclear states is poor, this is compensated for by the very much larger energy E_γ of the transition in the factor E_γ^3. The predicted branching to the $[0]p$ state is small, but that to the nuclear $[1]p$ or $[0]f$ states, $\sim 10^{-4}$, is comparable to that for the atomic $2p$ state. These transitions would result in a γ-ray line of about 42 MeV with a line width of about 35 MeV. The observation of such transitions would provide valuable evidence for the nature of the $\bar{p}$-nuclear potential.

TABLE III. Limits of n-$\bar{n}$ oscillation time $\tau_{n\bar{n}}$ as determined by the different potentials for ^{16}O.

Potential	V (MeV)	W (MeV)	Limits (sec)
S	198	30.4	$\tau_{n\bar{n}} > 1.4 \times 10^7$
S'	367	34.0	$\tau_{n\bar{n}} > 6.6 \times 10^6$
D	86	161.0	$\tau_{n\bar{n}} > 2.6 \times 10^7$

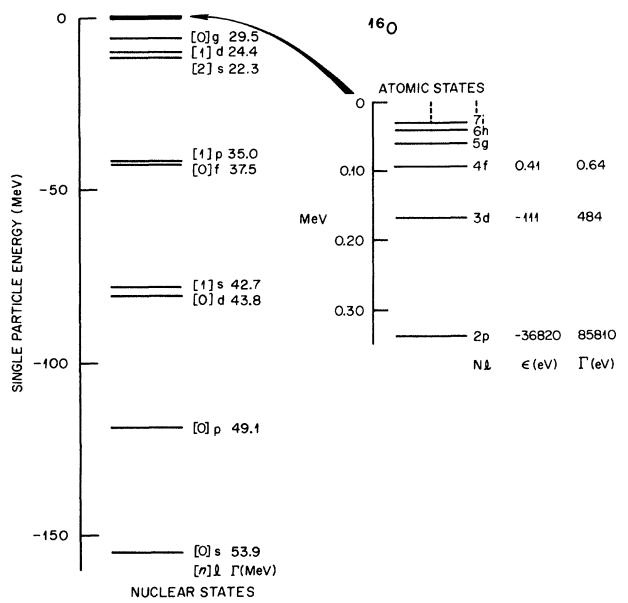

FIG. 4. Single-particle levels for $\bar{p}+^{16}O$ using the S potential of Table I. The atomic states are shown on an expanded scale to the right. Also shown are the shifts ϵ and the widths Γ of some of the states.

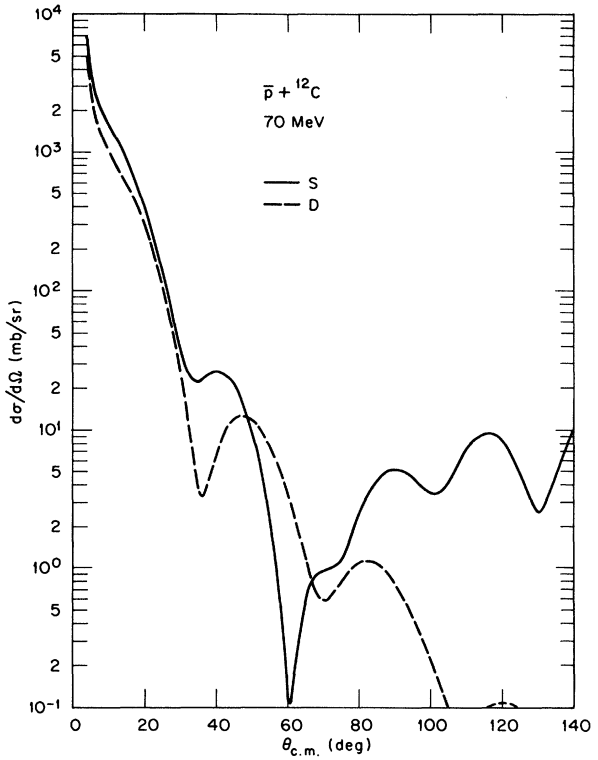

FIG. 5. Differential cross sections for $\bar{p}+^{12}C$ elastic scattering at a bombarding energy of 70 MeV, calculated using the S- and D-type potentials of Table I.

D. Antiproton-nucleus scattering

The differential cross sections for the scattering of antiprotons by nuclei have to be measured in order to learn the details of the $\bar{p}$-nucleus potential. Such experiments are planned for the LEAR facility at CERN. Scattering experiments must, however, be done at positive energies, sufficiently high that the scattering is sensitive to the shape of the potential. Thus, one also needs to know the energy dependence of the potential in order to relate scattering and bound-state data. For example, other nonelastic channels are open at positive energies and this leads to an increase in the absorptive potential. However, our purpose here is to look for any indication that scattering measurements could help to distinguish the S and D potential sets deduced from the $\bar{p}$-atom data.

Calculations were made for a bombarding energy of 70 MeV. The S potentials predict much larger elastic cross sections at large angles, as Fig. 5 shows for $\bar{p}+^{12}C$, than do the D potentials. This is like the result obtained by Auerbach *et al.*,[12] although we see here that it is not necessary to have the real potential radius be greater than the imaginary one in order to enhance the large-angle cross sections. Rather, it is a consequence of the small W/V ratio, which is ~ 0.1 for the S sets but $\gtrsim 1$ for the D sets. On the other hand, the reaction (or absorption) cross sections σ_A are rather similar for the two potential families. Table V gives values for σ_A and also the elastic cross sections σ_{el} integrated for $\theta \geq \theta_{min}$. Calculations using the limits shown in Fig. 1 suggest uncertainties of order 20%

TABLE IV. Transition widths for $E1$ decay of the $3d$ atomic state of $\bar{p}+^{16}O$ which has a binding energy of 0.167 MeV.

Final state	Binding energy (MeV)	Γ_{E1} (eV)	$\Gamma_{E1}/\Gamma_{total}$
$2p$ atomic	0.339	0.25	5.2×10^{-4}
$[1]p$ nuclear	41.98	0.099	2.1×10^{-4}
$[0]f$ nuclear	42.69	0.060	1.2×10^{-4}
$[0]p$ nuclear	118.4	0.004	7.5×10^{-6}

TABLE V. Absorption (or reaction) cross sections σ_A and integrated elastic cross sections σ_{el} for $\bar{p}$+nucleus scattering at 70 MeV, using the potentials of Table I.

Nucleus	Potential	σ_A (mb)	$\sigma_{el}(\theta_{min})^a$ (mb)	θ_{min} (deg)
^{12}C	S	511	606	4.5
	D	496	387	4.5
^{16}O	S	531	636	6
	S'^b	609	635	6
	D	646	396	6
^{32}S	S	919	937	6
	D	928	677	6
^{89}Y	S	1495	2118	6
	D	1756	1434	6

[a]Elastic differential cross section integrated over $\theta_{min} \leq \theta \leq 180°$.
[b]See text.

in these numbers owing to uncertainties in the $\bar{p}$-atom data.

Measurements[14] on ^{12}C at ~ 70 MeV give $\sigma_A = 730 \pm 180$ mb. Both the predicted σ_A values and their associated uncertainties can be represented as 500 ± 100 mb. Although somewhat lower than the measured value, they overlap within their errors. As Fig. 5 indicates, differential cross section measurements could give a more definitive answer, while Table V shows that even the integral elastic cross section could easily distinguish between the two potentials. For $\theta_{\min} = 4.5°$, the prediction for S is 60% larger than for D.

A cross section for ^{208}Pb was also deduced from these measurements,[14] $\sigma_A = 5.3 \pm 1.7$ b. Data on the $\bar{p}$-atom for Pb are not available, but we made a rough extrapolation from the potentials given in Table I. Both S- and D-type potentials yield σ_A of about 3 b. The predicted σ_A are much smaller than the measured one. Indeed, exploratory calculations[15] suggest that it would be difficult to find a "reasonable" optical potential which would give such a large reaction cross section.

Other measurements of σ_A are available[16] for energies of 118 and 174 MeV. Those for ^{12}C are (410 ± 35) mb and (422 ± 25) mb, respectively. The predictions for both S and D potentials are in reasonable agreement with these values, with the S agreeing exactly at 118 MeV and the D agreeing exactly at 174 MeV. More extensive studies of elastic and inelastic scattering will be presented elsewhere.[15]

E. Summary

Four representative cases of $\bar{p}$-atom data were examined, and $\bar{p}$-nucleus potentials deduced. It was assumed that these potentials had shapes which followed the density distributions of the nuclei. There is not a unique potential to fit the data for each nucleus, but two families of complex strengths were found (Table I), the D type with deep absorptive strength ($W \sim 100-200$ MeV) and a relatively shallow real potential ($V \sim 100$ MeV), and the S type, with a shallow imaginary potential ($W \sim 15-45$ MeV) and deep real part ($V \sim 200-360$ MeV).

Some possible consequences of the differences between these two potential families were examined. For example, the observed stability of nuclei implies an n-$\bar{n}$ oscillation time several times smaller when the S potentials are used than when the D potentials are assumed. The S potentials also suggest the possibility of observing $\bar{p}$-nuclear bound states, whereas the D type implies that these are too broad to be seen. The two potential types also give rise to different elastic scattering characteristics; the S potentials predict much larger differential cross sections at large angles (Fig. 5), but the two families imply similar absorption (or reaction) cross sections. Those predicted for $\bar{p} + {}^{12}C$ at 118 and 174 MeV are in agreement with the measurements,[16] although the predictions at 70 MeV are lower than the measured values.[14] Indeed, the cross section reported for $\bar{p} + {}^{208}Pb$ at 70 MeV cannot be understood in terms of a simple potential model.

ACKNOWLEDGMENTS

The authors wish to thank Prof. M. Goodman, Prof. E. Lomon, Prof. E. Moniz, Prof. R. Seki, and Dr. P. Mulders and Dr. R. Martin for helpful discussions. This research was sponsored in part by the Division of Basic Energy Sciences, U.S. Department of Energy, under Contract No. DE-AC02-76 ER0 3069 with M.I.T., and Contract No. W-7405-eng-26 with the Union Carbide Corporation.

APPENDIX: BOUND STATE FOR A COMPLEX POTENTIAL

The Schrödinger equation for the radial wave function $u(r)$ is

$$\left[-\frac{d^2}{dr^2} - \frac{l(l+1)}{r^2} + \frac{2\mu}{\hbar^2}\left[\frac{Z_1 Z_2 e^2}{r} + U(r)\right] - E\right] u(r) = 0 .$$

Although strictly speaking the Coulomb potential from a finite charge distribution should be used here, we are only concerned with the *differences* between eigenvalues with and without the nuclear potential $U(r)$. These differences are known[1] to be insensitive to the form of the Coulomb potential. Near the origin the wave function behaves as

$$u(r) \sim r^{l+1} ,$$

and at distances far from the nuclear radius it behaves as

$$u(r) \sim \rho^{l+1} e^{-\rho/2} U(-N+l+1, 2l+2, \rho) ,$$

where $U(\alpha, \beta, \rho)$ is the Kummer function.[17] The dimensionless but complex quantities ρ and N are related to the Bohr radius a and energy unit E_0 by

$$\rho = \frac{2r}{Na} ,$$

$$N = \sqrt{-E/2E_0} ,$$

$$a = \frac{\hbar^2}{|Z_1 Z_2| e^2 \mu} ,$$

and

$$E_0 = \mu (Z_1 Z_2 e^2/\hbar)^2 .$$

A numerical program for the Kummer function was written to give the Coulomb wave function for complex N and ρ. The wave function is then integrated inward from about 10 fm distance away from the nuclear radius. The wave function is also integrated outward from the origin and the two are matched at a distance near the nuclear radius. As the logarithmic derivative can become very large near a nodal point, it is sometimes necessary to change the matching radius in order to obtain the eigenenergies.

In the case of a complex square well $-(V + iW)\theta(R - r)$ joined onto an attractive Coulomb potential, the eigenvalue equation can be written out explicitly and its numerical solution provides a useful check for the numerical integration procedures:

$$\kappa R\frac{j_l'(\rho_1)}{j_l(\rho_1)}=\frac{2}{N}\left[\frac{l}{\rho}-\frac{1}{2}+\frac{U'(-N+l+1,2l+2,\rho)}{U(-N+l+1,2l+2,\rho)}\right],$$

where

$$\kappa=[2\mu(E+V+iW)/\hbar^2]^{1/2}$$

and

$$\rho_1=\kappa R\ .$$

---

*Permanent address: Oak Ridge National Laboratory, Oak Ridge, TN 37830.

†Permanent address: University of Kentucky, Lexington, KY 40506.

[1]R. Seki and C. E. Wiegand, Annu. Rev. Nucl. Sci. 25, 241 (1975); C. J. Batty, Fiz. Elem. Chastits At. Yadra 13, 164 (1982) [Sov. J. Part. Nucl. 13, 71 (1982)].

[2]R. Roberson, T. King, R. Kunselman, J. Miller, R. J. Powers, P. D. Barnes, R. A. Eisenstein, R. B. Sutton, W. C. Lam, C. R. Cox, M. Eckhause, J. R. Kane, A. M. Rushton, W. F. Vulcan, and R. E. Welsh, Phys. Rev. C 16, 1945 (1977); P. D. Barnes, S. Dytman, R. A. Eisenstein, W. C. Lam, J. Miller, R. B. Sutton, D. A. Jenkins, R. J. Powers, M. Eckhause, J. R. Kane, B. L. Roberts, R. E. Welsh, A. R. Kunselman, R. P. Redwine, and R. E. Segel, Phys. Rev. Lett. 29, 1132 (1972).

[3]H. Poth, G. Backenstoss, I. Bergstrom, P. Blum, J. Egger, W. Fetscher, R. Guigas, R. Hagelberg, N. Hassler, C. J. Herrlander, M. Izycki, H. Koch, A. Nilsson, P. Pavlopoulos, H. P. Povel, K. Roslhi, I. Sick, L. Simons, A. Schwitter, J. Stzarkier, and L. Tauscher, Nucl. Phys. A294, 435 (1978).

[4]C. J. Batty, Nucl. Phys. A372, 433 (1981).

[5]A. M. Green and S. Wycech, Nucl. Phys. A377, 441 (1982); A. M. Green, W. Stepien-Rudzka, and S. Wycech, *ibid.* A399, 307 (1983).

[6]T. Suzuki and H. Narumi, Phys. Lett. 125B, 251 (1983).

[7]A. Bouyssy and S. Marcos, Phys. Lett. 114B, 397 (1982).

[8]J. Boguta, Phys. Lett. 106B, 245 (1981).

[9]For a recent review, see Proceedings of the Informal Workshop on Neutron-Antineutron Oscillations, edited by M. S. Goodman, M. Machacck, and P. D. Miller, Harvard University report 1982; P. G. Sandars, J. Phys. G 6, L161 (1980); Riazuddin, Phys. Rev. D 25, 885 (1982); W. M. Alberico, A. Bottino, and A. Molinari, Phys. Lett. 114B, 266 (1982).

[10]C. B. Dover, A. Gal, and J. M. Richard, Phys. Rev. D 27, 1090 (1983).

[11]H. Koch, in *Proceedings of the Fifth International Conference on High Energy Physics and Nuclear Structure,* edited by G. Tibell (North-Holland, Amsterdam, 1975).

[12]E. H. Auerbach, C. B. Dover, and S. H. Kahana, Phys. Rev. Lett. 46, 702 (1981).

[13]M. L. Cherry, K. Lande, C. K. Lee, R. I. Steinberg, and B. Cleveland, Phys. Rev. Lett. 50, 1354 (1983); P. K. Kabir, *ibid.* 51, 231 (1983).

[14]H. O. Cohn, J. E. Brau, W. M. Bugg, G. T. Condo, T. Handler, and E. L. Hart (unpublished).

[15]A. D. MacKellar, G. R. Satchler, and C. Y. Wong (unpublished).

[16]H. Aihara, J. Chiba, H. Fujii, T. Fujii, H. Iwasaki, T. Kamae, K. Nakamura, T. Sumiyoshi, Y. Takada, T. Takeda, M. Yamauchi, and H. Fukuma, Nucl. Phys. A360, 291 (1981).

[17]M. Abramowitz and I. A. Stegun, *Handbook of Mathematical Functions* (Dover, New York, 1965), p. 504, Eq. (13.1.6).